

2009

Electromagnetic Induction Sensor Data to Identify Areas of Manure Accumulation on a Feedlot Surface

Bryan Woodbury
USDA-ARS, bryan.woodbury@ars.usda.gov

Scott M. Lesch
Univ. of California

Roger A. Eigenberg
USDA-ARS, roger.eigenberg@ars.usda.gov

Daniel N. Miller
University of Nebraska-Lincoln, dan.miller@ars.usda.gov

Mindy J. Spiehs
USDA-ARS, U.S. Meat Animal Research Center, mindy.spiehs@ars.usda.gov

Follow this and additional works at: <https://digitalcommons.unl.edu/hruskareports>

Woodbury, Bryan; Lesch, Scott M.; Eigenberg, Roger A.; Miller, Daniel N.; and Spiehs, Mindy J., "Electromagnetic Induction Sensor Data to Identify Areas of Manure Accumulation on a Feedlot Surface" (2009). *Roman L. Hruska U.S. Meat Animal Research Center*. 362.
<https://digitalcommons.unl.edu/hruskareports/362>

This Article is brought to you for free and open access by the U.S. Department of Agriculture: Agricultural Research Service, Lincoln, Nebraska at DigitalCommons@University of Nebraska - Lincoln. It has been accepted for inclusion in Roman L. Hruska U.S. Meat Animal Research Center by an authorized administrator of DigitalCommons@University of Nebraska - Lincoln.

Electromagnetic Induction Sensor Data to Identify Areas of Manure Accumulation on a Feedlot Surface

Bryan L. Woodbury*

USDA-ARS
U.S. Meat Animal Research Center
P.O. Box 166
Clay Center, NE 68933

Scott M. Lesch

Dep. of Environmental Science
Univ. of California
Riverside, CA 92521

Roger A. Eigenberg

USDA-ARS
U.S. Meat Animal Research Center
P.O. Box 166
Clay Center, NE 68933

Daniel N. Miller

USDA-ARS
Agroecosystem Management Unit
104 Chase Hall
Univ. of Nebraska, East Campus
Lincoln, NE 68583

Mindy J. Spiels

USDA-ARS
U.S. Meat Animal Research Center
P.O. Box 166
Clay Center, NE 68933

A study was initiated to test the validity of using electromagnetic induction (EMI) survey data, a prediction-based sampling strategy, and ordinary linear regression modeling to predict spatially variable feedlot surface manure accumulation. A 30- by 60-m feedlot pen with a central mound was selected for this study. A Dualem-1S EMI meter (Dualem Inc., Milton, ON, Canada) pulled on 2-m spacing was used to collect feedlot surface apparent electrical conductivity (EC_a) data. Meter data were combined with global positioning system coordinates at a rate of five readings per second. Two 20-site sampling approaches were used to determine the validity of using EMI data for prediction-based sampling. Soil samples were analyzed for volatile solids (VS), total N (TN), total P (TP), and Cl^- . A stratified random sampling (SRS) approach ($n = 20$) was used as an independent set to test models estimated from the prediction-based ($n = 20$) response surface sample design (RSSD). The RSSD sampling plan demonstrated better design optimality criteria than the SRS approach. Excellent correlations between the EMI data and the $\ln(Cl^-)$, TN, TP, and VS soil properties suggest that it can be used to map spatially variable manure accumulations. Each model was capable of explaining >90% of the constituent sample variations. Fitted models were used to estimate average manure accumulation and predict spatial variations. The corresponding prediction maps show a pronounced pen design effect on manure accumulation. This technique enables researchers to develop precision practices to mitigate environmental contamination from beef feedlots.

Abbreviations: EC_a , apparent electrical conductivity; EMI, electromagnetic induction; GPS, global positioning system; LR, linear regression; RSSD, response surface sampling design; SRS, stratified random sampling; TN, total nitrogen; TP, total phosphorus; VS, volatile solids.

Management and control of accumulated manure has become an important issue for feedlot operators. Increasing costs for environmental compliance and decreasing profit margins have forced producers to reevaluate their management prac-

tics. Manure accumulation in the pen is not uniform across the entire surface. The quantity and quality of the manure pack is dependent on many variables, such as length of accumulation time, pen design, slope, climate, season, feed ration, stocking density, operator management, soil type, etc. (Bierman et al., 1999; Frecks and Gilbertson, 1974; Gilbertson et al., 1975; Kissinger et al., 2007; Sweeten et al., 1985). Understanding where manure accumulates on the surface and developing precision management practices that focus on these zones should improve efficiency in environmental protection and provide economic benefits.

Precise harvesting of manure can result in collected material that is much higher in volatile solids and lower in ash (i.e., soil) content than those obtained using traditional collection methods (Kissinger et al., 2007; Sweeten et al., 1985). Harvesting accumulated manure low in ash content can have other economical benefits beyond the volume and mass reductions. Harvesting a nutrient-rich material can increase the distances it can be economically hauled for land application. Another benefit could be realized in energy recovery through direct combustion at a coal-fired electric power plant (Annamalai et al., 2003; Priyadarsan et

Mention of trade names or commercial products in this publication is solely for the purpose of providing specific information and does not imply recommendation or endorsement by the U.S. Department of Agriculture.

Soil Sci. Soc. Am. J. 73:2068-2077
doi:10.2136/sssaj2008.0274

Received 20 Aug. 2008.

*Corresponding author (bryan.woodbury@ars.usda.gov).

© Soil Science Society of America

677 S. Segoe Rd. Madison WI 53711 USA

All rights reserved. No part of this periodical may be reproduced or transmitted in any form or by any means, electronic or mechanical, including photocopying, recording, or any information storage and retrieval system, without permission in writing from the publisher. Permission for printing and for reprinting the material contained herein has been obtained by the publisher.

al., 2004). Recent work by Sweeten et al. (2006) found that the higher heating value of feedlot surface material harvested from soil surface pens had approximately 30% of the higher heating value per equivalent weight of Powder River basin coal when soil particles were entrained; however, material harvested from fly-ash-surfaced pens was approximately 62% of the higher heating value per equivalent weight when soil particles were eliminated.

Greenhouse gases and malodorous compounds like volatile fatty acids, aromatics, sulfides, amides, and alcohols are emitted from accumulated manure; therefore, considerable research has gone into measuring gas emissions from feedlots (Auvermann et al., 2007; Ham and Baum, 2007; Kyoung et al., 2007; Todd et al., 2008). Flux chambers and wind tunnels have been used to estimate emissions at specific points on a feedlot surface (Duysen et al., 2003; Meisinger et al., 2001). Unfortunately, these methods are not adequate to predict large area emissions, particularly when there is considerable spatial variability. More complicated approaches using micrometeorological theories with various measurement technologies have been used effectively for measuring emission from large surfaces (Flesch et al., 2005, 2007; Harper et al., 1999; McGinn et al., 2003; Todd et al., 2005). These methods lack the resolution necessary to develop precision management practices for mitigating emissions.

Methods have been developed to measure soil conductivity (EC_a) using EMI. These methods have been used to correlate EC_a values with salts contained in animal manure (Eigenberg et al., 2002, 2005; Eigenberg and Nienaber, 2003). Traditional methods for using covariate information to estimate the spatial distribution of specific ionic constituents use techniques like cokriging (Isaaks and Srivastava, 1989) or kriging with external drift (Wackernagel, 1998). These techniques can be effective but usually require many samples to get adequate estimates on key statistical parameters. An alternative to these methods, using multilinear regression, has been used extensively for describing salt-affected irrigated soils (Corwin and Lesch, 2005; Lesch, 2005; Rhoades et al., 1999; Lesch et al., 1995a,b). This method uses EMI soil conductivity survey data to identify sample locations for a calibration set. The calibration data are then combined with the EMI survey data to determine an appropriate linear regression model. Recently, Eigenberg et al. (2008) successfully adapted these techniques to describe the spatial distribution of Cl^- contained in runoff to a vegetative treatment area.

The overall objective of this project was to test the validity of using EMI survey data in conjunction with a prediction-based sampling strategy and ordinary linear regression modeling techniques to measure and predict spatially variable manure accumulation on a feedlot surface. Information from this study will be used to develop precision feedlot management practices that improve the efficiency of envi-

ronmental mitigation by the feedlot operators. For this project, our specific research objectives were to: (i) assess the accuracy of a prediction-based sampling strategy, in comparison with an SRS procedure for calibrating suitable EMI–soil property regression equations; (ii) test the ability of a regression model estimated via use of a prediction-based sampling strategy to accurately predict spatial manure accumulation at randomly chosen validation sites on the feedlot surface; (iii) evaluate feedlot surface data for any spatial structure in the manure accumulation; (iv) begin to establish a general methodology for measuring and monitoring spatially variable chemical constituents associated with manure accumulation on research- and commercial-sized feedlot pen surfaces; and (v) develop a method for interpreting the predicted spatial manure accumulation patterns on the feedlot surface and suggest application of this information to management practices.

MATERIALS AND SURVEY AND SAMPLING METHODS

Site

A 30- by 60-m pen at the U.S. Meat Animal Research Center near Clay Center, NE, was selected for this study (Fig. 1). The typical stocking density of this pen is approximately 24 m² per animal. The pens were constructed on top of a Hastings silt loam soil (a fine, smectitic, mesic

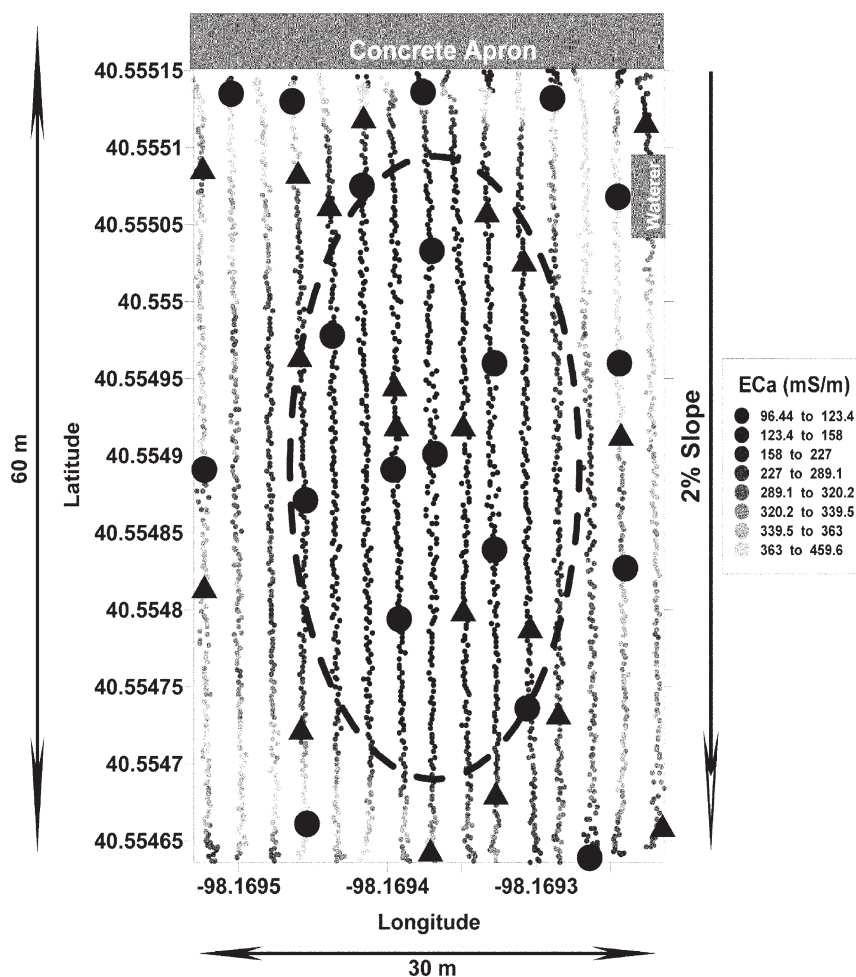


Fig. 1. Electromagnetic induction (EMI) survey data of the feedlot pen. Output is apparent electrical conductivity (EC_a). The circles represent the response surface sample design (RSSD) locations and the triangles represent the stratified random sampling (SRS) design locations. Note that the feed bunk is located on the north end of the pen, the oval is the central mound, and the waterer is located near the northeast corner of the pen.

Udic Argiustoll). The central mound was constructed with soil excavated from the C horizon of the same soil series at an offsite location. The C horizon is typified by a silt loam texture with free carbonates. Each pen surface is cleaned and reconditioned annually during July and August; however, periodic cleaning and removal of localized accumulated manure is done when needed between cleanings. Typical cleaning procedures include scraping and removing excess manure accumulation and reshaping the central mound. Also, any eroded areas not filled during the scraping process are filled in with the same soil used to shape the mound. The pen used for this study was stocked with approximately 75 head of cattle fed various combinations of corn (*Zea mays* L.)-based finish rations.

Feedlot Survey

Specific details on the EMI equipment and techniques used for this study are described in Eigenberg et al. (2005, 2008). Briefly, a Dualem-1S meter (Dualem Inc., Milton, ON, Canada) was used to collect EC_a data from the feedlot surface. The meter was positioned on a nonmetallic sled and manually pulled at approximately 1.5 m s^{-1} at 2-m intervals across the pen surface. Path spacing was maintained using a Trimble EZ-Guide global positioning system (GPS)-guidance system (Trimble Navigation Ltd., Sunnyvale, CA). The Dualem-1S meter simultaneously records both horizontal and vertical dipole modes; however, only the more shallow penetrating (depth-measured centroid at approximately 0.75 m) horizontal dipole mode was used for the statistical analysis. Simultaneously, GPS coordinates of the meter's position within the pen were determined using an AgGPS 332 receiver with OminiSTAR XP correction resulting in 10- to 20-cm accuracy (Trimble Navigation Ltd.). Coordinate and EC_a data were collected at a rate of five samples per second and stored in a Juniper System Allegro (Juniper Systems, Logan, UT) datalogger. Edge effects from metal fencing were clipped from the EC_a data set before the sampling designs were determined.

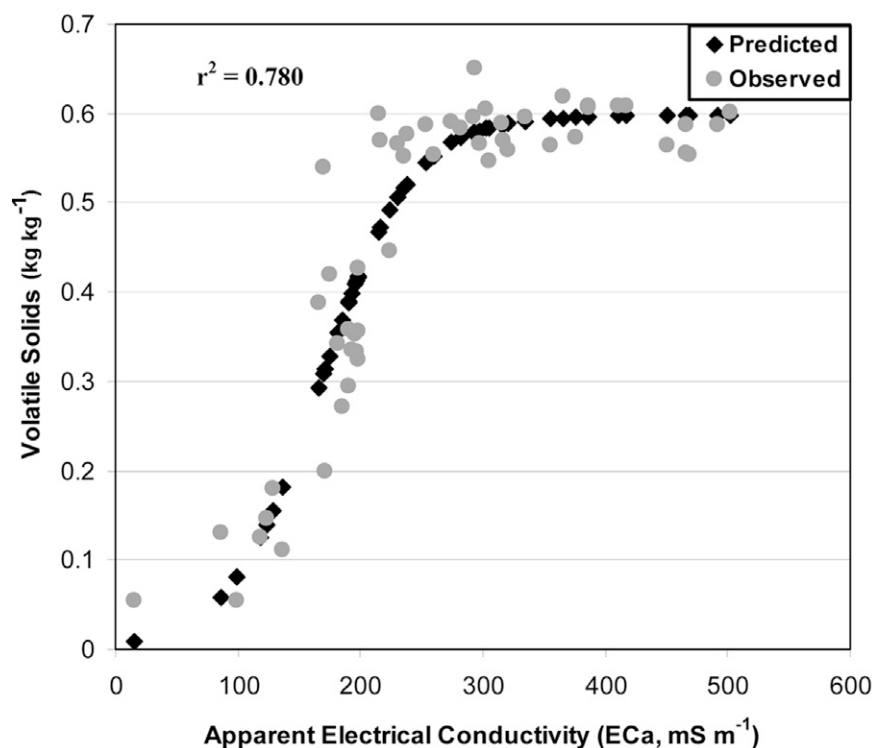


Fig. 2. Measured apparent electrical conductivity and the corresponding volatile solids content. Data represent a variety of feedlots in Nebraska and Texas.

Sampling Designs

Two sampling strategies, similar to those used by Eigenberg et al. (2008), were used to achieve the stated objectives. The basis for these sampling strategies is the strong correlation ($R^2 = 0.780$) between EC_a and VS illustrated in Fig. 2. Data in Fig. 2 are from multiple feedlots throughout the Midwest under varying climatic conditions and management styles. The strong correlation results from the EMI response to the high salt content of the manure pack. Also, the soil beneath the pack is relatively low and stable in conductivity. Additional justifications concerning the sampling procedures were given in Eigenberg et al. (2008). An SRS design was determined by ranking the pen EC_a data from the highest to lowest value. This ranking was segmented into four ranges with an equal number of values in each. Next, five values from each range ($n = 20$) were selected using a random number generator. The GPS coordinates associated with each selected value was used to navigate back to that location on the feedlot pen surface for sample collection. Another 20 sites were selected using the spatial RSSD program contained in the USDA-ARS ESAP (EC_c Sampling, Assessment, and Prediction) software package (Lesch et al., 2000). The GPS coordinates associated with the selected EC_a values were used to navigate back to these sites on the pen surface for sample collection.

The sampling approach incorporated into the ESAP software package is specifically designed for use with ground-based EC_a signal readings (Lesch, 2005). In this prediction-based sampling approach, a minimum set of calibration samples are selected based on the observed magnitudes and spatial locations of the EC_a data. These sites are chosen in an iterative, nonrandom manner to: (i) optimize the estimation of a regression model (i.e., minimize the mean square prediction errors produced by the calibration function); and (ii) simultaneously maximize the average separation distance between adjacent sampling locations (to reduce the possibility of observing spatially correlated residual errors). Intuitively, this sampling approach represents a hybrid mixture of a response surface sampling technique (Myers and Montgomery, 2002) with a space-filling algorithm (Müller, 2001). Lesch (2005) demonstrated that such a sampling approach can substantially outperform a probability-based sampling strategy with respect to a number of important model-based prediction criteria.

The use of two distinct sampling approaches allowed us to compare and contrast their performance in calibration of the EMI model. Additionally, the SRS plan was also used as an independent data set for testing the validity of the regression model (estimated from the prediction-based RSSD sample design). Three different regression model validation tests were used to assess the accuracy and reliability of the fitted model. These tests were used to verify that the regression model (estimated using data from just the RSSD sample sites) was capable of producing accurate and unbiased predictions at the independently chosen SRS sites. When performing these tests, the RSSD sample sites were treated as calibration sites, while the SRS sample sites were treated as validation sites.

Sample Collection and Analysis

Once the sampling designs were generated, pen surface material was collected to a depth of

10 cm at all 40 sites to determine the VS (loss-on-ignition method, Nelson and Sommers, 1996), TN (Dumas method, Bremner, 1996), TP (HClO₄ digestion, Kuo, 1996), and Cl⁻ using a Cl⁻ specific ion electrode (Frankenberger et al., 1996). These first three constituents were selected because VS is a measure of manure content, and TN and TP contained in the manure (i.e., feces and urine) are considered important nutrients in the environment. Chloride was included because it is useful as an indicator to measure potential salt movement in the environment. The unconsolidated surface material in a 15-cm radius around each sample site was collected and stored in a 4-L plastic bag. Next, a hand-held pick was used to remove the soil–manure pack material below the unconsolidated surface material to an approximate depth of 10 cm, which was then stored in the same bag. Pen surface material was air dried and mechanically ground to pass through a 2-mm sieve.

STATISTICAL METHODOLOGY

Several methods have been developed to collect high-density EC_a data; however, soil samples for use in calibration must normally be collected at a certain number of corresponding EC_a survey locations. The measured salt or soil properties associated with these soil samples are then used (in conjunction with the co-located survey data) to estimate some type of spatial-statistical or geostatistical model. This statistical model is in turn used to predict the detailed spatial soil property (salt or nutrient) pattern from the full set of acquired survey data.

One of the simplest and most frequently used statistical modeling approaches for calibrating EC_a survey information with various soil property measurements is ordinary regression. Ordinary regression models represent a special case of a much more general class of models commonly known as linear regression models with spatially correlated errors (Schabenberger and Gotway, 2005), hierarchical spatial models (Banerjee et al., 2004), or geostatistical mixed linear models (Haskard et al., 2007). This broader class of models includes many of the geostatistical techniques familiar to soil scientists, such as universal kriging and kriging with external drift, as well as standard regression techniques like ordinary linear regression (LR) models and analysis of covariance models.

Lesch et al. (1995a,b) suggested using a prediction-based sampling strategy in conjunction with ordinary regression modeling for predicting soil salinity from EC_a survey information. Lesch (2005) refined and extended this sampling methodology and suggested that this sampling approach might also be used to optimally estimate LR models for predicting other soil properties from EC_a signal data. We have adopted this approach for the current study, the goal being to use the EMI survey data to map the spatial manure accumulation on the feedlot surface. Note that the LR modeling approach is particularly advantageous in our current application, since a typical LR model can be estimated using a fairly small sample size, i.e., usually 10 to 20 sites (Lesch, 2005). Additionally, it is well known that a kriging with external drift model reduces exactly to an ordinary LR model when the model residuals are spatially uncorrelated (Schabenberger and Gotway, 2005). Likewise, a cokriging model also reduces to a LR model (at all locations where survey data have been acquired) when the residuals are spatially uncorrelated (Lesch et al., 1995a).

Model Specification and Assumptions

A preliminary analysis of EMI–chemical property relationships revealed that all of the structural relationships were strongly curvilinear. Hence, the following spatially referenced, multivariate LR model was used to describe the relationships between the VS, TN, TP, and natural log transformed Cl⁻ [ln(Cl⁻)] data and the EMI [ln(EMI)] signal data:

$$y_{ij} = \beta_{0j} + \beta_{1j} \ln(\text{EMI}_i) + \beta_{2j} [\ln(\text{EMI}_i)]^2 + \varepsilon_{ij} \quad [1]$$

where y_{ij} represents the value of the j th chemical property at the i th sampling location, β_{0j} through β_{2j} represent unknown regression model parameters for the j th regression equation ($j = 1, 2, 3, 4$), and ε_{ij} represents the j th spatially uncorrelated random normal error component. Note that the logarithmic transformations were used to reduce the curvilinear EMI–chemical property relationships and stabilize the Cl⁻ regression model variance. In matrix notation, each of the four distinct regression models quantified by Eq. [1] can be conveniently expressed as

$$\mathbf{y} = \mathbf{XB} + \mathbf{e} \quad [2]$$

where \mathbf{y} represents the $(m \times 1)$ vector of the VS, TN, TP, or ln(Cl⁻) data, \mathbf{X} represents an $(m \times 3)$ fixed data matrix of the (linear and quadratic) log-transformed sensor readings, \mathbf{B} represents a (3×1) vector of unknown parameter estimates, and \mathbf{e} represents a vector of normally and independently distributed residual errors with variance σ^2 , e.g., $\mathbf{e} \sim N(0, \sigma^2 \mathbf{I})$, where \mathbf{I} represents the identity matrix. Note that this model implies that all four chemical property vs. EMI signal data relationships are best described by a quadratic function of the log-transformed EMI signal data.

A critical assumption in Eq. [2] is that the regression model errors are normally distributed and spatially uncorrelated. In practice, these residual error assumptions must be verified before using an ordinary LR model for prediction purposes. The Moran residual test statistic (Tiefelsdorf, 2000; Haining, 1990; Upton and Fingleton, 1985) was used to assess the validity of the uncorrelated error assumption. The Moran residual score (δ_M) is defined as

$$\delta_M = \frac{\mathbf{r}^T \mathbf{W} \mathbf{r}}{\mathbf{r}^T \mathbf{r}} \quad [3]$$

where $\mathbf{r} = \mathbf{y} - \mathbf{Xb}$ (i.e., the vector of observed model residuals), T is the matrix transcript operator, \mathbf{W} is a suitably specified proximity matrix, and $\mathbf{b} = (\mathbf{X}^T \mathbf{X})^{-1} \mathbf{X}^T \mathbf{y}$. In this analysis, \mathbf{W} was defined to be a scaled inverse distance squared matrix; i.e., the $\{w_{ij}\}$ elements associated with the i th row of this matrix were defined as

$$w_{ii} = 0 \text{ and } w_{ij} = \frac{d_{ij}^{-2}}{\sum_{j=1}^n d_{ij}^{-2}} \quad [4]$$

where d_{ij} represents the computed distance between the i th and j th sample locations. The Moran test score was then computed as

$$S_M = \frac{\delta_M - E(\delta_M)}{\sqrt{\text{Var}(\delta_M)}} \quad [5]$$

where the expectation and variance of the test statistic were computed using the formulas given in Lesch and Corwin (2008). Additionally, the normality assumption was assessed using standard residual quantile–quantile plots and the Shapiro–Wilk test (Myers, 1986; Shapiro and Wilk, 1965).

Sample Design Optimality Criteria

For a hypothesized ordinary LR model, various statistical criteria have been proposed in the response surface design literature for assessing the “optimality” of competing sampling designs (Myers and Montgomery, 2002). Most of these criteria measure either the expected precision of the regression model parameter estimates (e.g., D and A optimality) or quantify some measure of precision in the model

Table 1. Basic electromagnetic induction (EMI) survey data and soil property summary statistics.

Variable†	Design‡	N or n	Mean	SD	Min.	Max.
EMI (shallow), mS m ⁻¹		2825	260.67	96.31	96.44	459.58
ln(EMI) (shallow), ln(mS m ⁻¹)		2825	5.480	0.431	4.569	6.130
Cl ⁻ , mg kg ⁻¹	RSSD	20	2763.3	1153.3	1237.0	4177.0
	SRS	20	2939.9	809.2	1487.0	3966.0
ln(Cl ⁻), ln(mg kg ⁻¹)	RSSD	20	7.829	0.463	7.120	8.337
	SRS	20	7.936	0.335	7.305	8.286
TN, mg kg ⁻¹	RSSD	20	13645.7	6471.4	1454.0	19500.0
	SRS	20	14734.5	5013.6	3036.0	19460.0
TP, mg kg ⁻¹	RSSD	20	4302.4	1966.7	915.0	6290.0
	SRS	20	4661.5	1571.6	1215.0	6262.0
VS, %	RSSD	20	31.56	15.11	4.91	46.10
	SRS	20	33.92	12.10	8.26	45.33

† TN, total N; TP, total P; VS, volatile solids.

‡ RSSD, response surface sampling design; SRS, stratified random sampling.

predictions (i.e., G, V, and Q optimality). In this study, we chose to compare and contrast the RSSD and SRS designs using the D-, V-, and G-optimality criteria; details concerning how each criteria are computed are presented in the Appendix.

In the current study, the D_{opt} , V_{opt} , and G_{max} scores associated with Eq. [2] were computed for each sampling design. Note that since the same general quadratic regression model structure was used to describe each of the four EMI-soil property relationships, the above scores needed to be computed just once (for each sampling design).

Individual and Field-Average Prediction Formulas

Relatively simple formulas for both individual and field-average prediction estimates can be immediately derived from standard linear modeling theory, provided that $\mathbf{e} \sim N(0, \sigma^2 \mathbf{I})$ and the assumed model is correct. More specifically, each individual prediction of the soil property (\hat{y}_{ij}) and its corresponding variance estimate ($\text{Var}\{y_{ij} - \hat{y}_{ij}\}$) were calculated as

$$\hat{y}_{ij} = \mathbf{x}_i^T \mathbf{b}_j$$

$$\text{Var}\{y_{ij} - \hat{y}_{ij}\} = s_j^2 \left[\mathbf{1} + \mathbf{x}_i^T (\mathbf{X}^T \mathbf{X})^{-1} \mathbf{x}_i \right] \quad [6]$$

where s_j^2 represents the estimated regression model mean square error for the j th soil property equation (Myers, 1986). These individual soil property predictions were then used to create spatial soil property maps of the surveyed feedlot. Likewise, field-average predictions (based on the entire survey grid) were computed as

$$\hat{y}_{\text{avg},j} = \mathbf{x}_{\text{avg}}^T \mathbf{b}_j$$

$$\text{Var}\{y_{\text{avg},j} - \hat{y}_{\text{avg},j}\} = s_j^2 \left[1/N + \mathbf{x}_{\text{avg}}^T (\mathbf{X}^T \mathbf{X})^{-1} \mathbf{x}_{\text{avg}} \right] \quad [7]$$

Table 2. Soil property correlation matrix, and soil property-electromagnetic induction (EMI) cross-correlation estimates.

	ln(Cl ⁻)	Total N	Total P	Volatile solids
Soil property correlation ($n = 40$)				
ln(Cl ⁻)	1.000	0.898	0.924	0.913
Total N		1.000	0.985	0.987
Total P			1.000	0.978
Volatile solids				1.000
Soil property-EMI cross-correlation estimates ($n = 40$)				
EMI	0.931	0.863	0.865	0.881
ln(EMI)	0.966	0.924	0.930	0.937

where \mathbf{x}_{avg} represents the average regression vector associated with all of the survey locations.

Model Validation

Three statistical tests were used to assess the validity of each estimated LR model: a composite-model F test, a joint-prediction F test, and a mean-prediction t -test. All three of these tests exploit the fact that the full set of sample data could be split into two disjoint sets, i.e., a primary calibration set (the RSSD design) and a secondary validation set (the SRS design). Each of these tests can be developed from general linear modeling theory and were described in more detail in Lesch and Corwin (2008).

Intuitively, the composite-model F test represents a test for parameter equivalence across the partitioned calibration and prediction (validation) data sets. In contrast, the joint-prediction F test assesses the ability of the regression model (fit using the calibration data only) to make unbiased predictions at all new validation sites and simultaneously tests if these prediction errors are within the specified tolerance (precision) of the estimated model. The mean-prediction t -test follows from the joint-prediction F test; this test can be used to determine if the predicted average value (across all n_2 validation sites) is unbiased.

RESULTS

The basic EMI survey and soil property summary statistics are presented in Table 1. The shallow EMI signal data exhibited a mean of 260.67 mS m⁻¹, a standard deviation of 96.31 mS m⁻¹, and a range from 96.4 to 459.6 mS m⁻¹. A histogram of the signal data (not shown) revealed that the sensor readings exhibited a bimodal data distribution. Gray-scale maps of the acquired EMI signal data are shown in Fig. 1 (along with the sampling positions for the two sampling plans). The average levels of the four soil properties (Cl⁻, TN, TP, and VS) were roughly equivalent across the two sampling plans (RSSD and SRS designs), but the observed standard deviations were consistently larger for the RSSD design (Table 1). This latter effect is a direct result of the nonrandom sampling strategy used in the RSSD algorithm (Lesch, 2005). More specifically, this algorithm selects more samples near the extremes of the signal data distribution, resulting in larger observed variance response variables (if and when the response variable[s] are strongly correlated with the EMI survey data).

The soil property correlation matrix and soil property-EMI cross-correlation estimates are both presented in Table 2. The TN, TP, and VS measurements were all very strongly correlated with one another; the ln(Cl⁻) measurements had correlations of approximately 0.9 with these other three variables. The cross-correlation estimates (lower portion of Table 2) suggest that each soil property exhibits a stronger correlation with the natural log transformed EMI signal than the raw EMI signal readings. Figures 3a and 3b show the ln(Cl⁻) vs. ln(EMI) and TN vs. ln(EMI) scatter plots, respectively. The ln(Cl⁻)-ln(EMI) relationship is nearly linear; the TN, TP, and VS measurements exhibit much more pronounced (and almost equivalent) curvilinear relationships with the ln(EMI) data.

Table 3 displays the quadratic regression model summary statistics and residual error tests for the models fit to the pooled

sample data ($n = 40$ sites). The four model R^2 values range from 0.91 to 0.94. In the TN, TP, and VS equations, all linear and quadratic parameter estimates were highly significant ($P < 0.001$). In the $\ln(\text{Cl}^-)$ equation, the linear and quadratic parameter estimates were significant below the $\alpha = 0.05$ level. Additionally, all four residual distributions passed both the Moran test and Shapiro–Wilk normality test at the $\alpha = 0.05$ significance level.

These fitted regression equations were, in turn, used to produce point estimates of the four soil properties across the entire EMI survey grid; Fig. 4 and 5 show the corresponding interpolated spatial $\ln(\text{Cl}^-)$ and VS maps, respectively. (The TN and TP maps appear to be nearly identical to the VS map, and are thus not shown.) All four maps clearly reflect the pen design (Fig. 1), exhibiting reduced levels of manure constituents on the mound and increasing levels around the edges of the feedlot. These same fitted equations were also used to estimate the average chemical constituent levels across the feedlot using Eq. [7]. These average prediction estimates (and 95% confidence intervals) were as follows: $\ln(\text{Cl}^-)$, 7.933 (7.899, 7.967); TN/1000, 15.14 (14.54, 15.74); TP/1000, 4.79 (4.63, 4.95); and VS, 34.86 (33.50, 36.21).

Table 4 shows the design optimality scores associated with each sampling plan. All three scores imply that the use of the RSSD design should lead to more accurate regression model parameter estimates and grid predictions. Specifically, the V_{opt} and G_{max} scores suggest that the average and maximum grid prediction errors should be about 4.7 and 38.1% less, respectively, for the RSSD design compared with the SRS design.

Table 5 displays the four sets of quadratic regression model summary statistics and individual parameter estimates for each sampling design. In general, summary statistics and parameter estimates were similar across designs. The composite-model F test results (Table 6) suggest that these parameter estimates are statistically equivalent (across designs); note that all four F tests are nonsignificant. All four joint-prediction F tests shown in Table 6 also exhibit nonsignificant test results. These latter results suggest that the regression models (fit using the RSSD sample data) can be used to make accurate and unbiased individual grid predictions at the randomly chosen SRS (validation) sites. Finally, the TN, TP, and VS mean-prediction t -tests also produced clearly nonsignificant results. Overall, only one out of 12 tests was found to be significant at the 0.05 level [the mean-prediction t -test associated with the $\ln(\text{Cl}^-)$ model] and none of the 12 model validation tests were significant at the 0.01 level.

DISCUSSION

Statistical Issues

The excellent correlations achieved in this study between the shallow EMI signal data and the $\ln(\text{Cl}^-)$, TN, TP, and VS soil properties confirm that EMI survey data can be effectively used to map spatially variable manure constituents in this pen feedlot, and suggest that this assessment methodology should be more broadly applicable. Each of the four quadratic regression models was capable of explaining >90% of the variation in the various constituent samples. The fitted regression models were, in turn, used to estimate the average accumulation levels and accurately predict the spatial variation in each component. The corresponding prediction maps clearly show the pronounced pen design effect on manure accumulation.

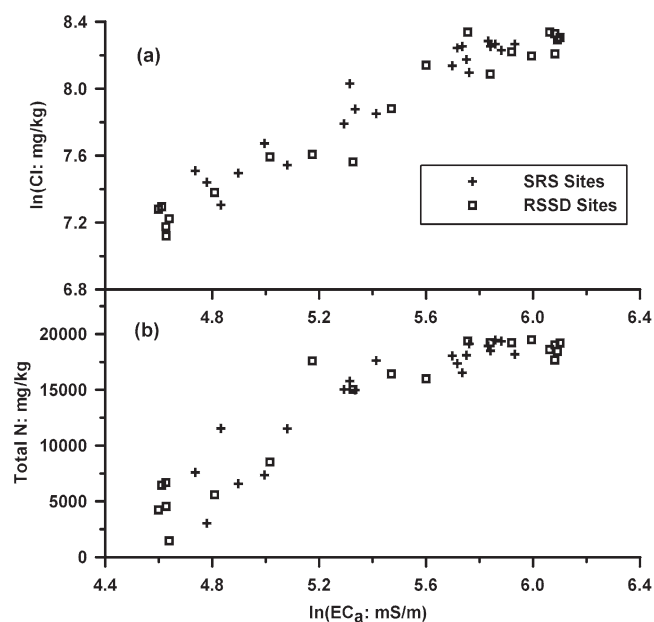


Fig. 3. Relationship between (a) $\ln(\text{Cl}^-)$ vs. $\ln(\text{apparent electrical conductivity, } EC_a)$ data, and (b) total N vs. $\ln(EC_a)$. Both the response surface sampling design (RSSD) and stratified random sampling (SRS) designs are represented in each plot.

When applicable, the primary advantage of using a regression modeling approach rather than more elaborate geostatistical modeling techniques is that far fewer calibration soil samples generally need to be acquired. In this study, the model validation results shown in Tables 5 and 6 suggest that accurate prediction equations could be estimated using a sample size of just $n = 20$ sites. When the SRS sample data were used as independent validation sites, 11 of the 12 model validation tests produced nonsignificant test results at the 0.1 significance level. Additionally, while either a probability-based (SRS) or a prediction-based (RSSD) design can be used to estimate the regression model(s), the optimality scores presented in Table 4 suggest that the RSSD design should lead to more accurate parameter estimates and model predictions. These results are consistent with previous studies that have compared these two sampling approaches (Eigenberg et al., 2008; Lesch, 2005).

Feedlot Management Strategies

Manure accumulation can impact the environment in many different ways, such as odor and greenhouse gas emissions, as nutrient runoff, as a pathogen source to human food supplies, and as a medium for insect development. Suitably calibrated EC_a survey data can help researchers better understand the pattern of manure accumulation on a given feedlot surface. This under-

Table 3. Quadratic regression model summary statistics and residual error tests ($n = 40$, pooled sample data).

Variable†	Model R^2	RMSE	Moran's residual		Shapiro–Wilk	
			Score	$P > F$	Score	$P > F$
$\ln(\text{Cl}^-)$	0.941	0.101	0.11	0.456	0.973	0.459
TN/1000	0.909	1.774	1.41	0.079	0.965	0.248
TP/1000	0.933	0.471	-0.10	>0.5	0.992	>0.5
VS	0.918	3.986	0.98	0.164	0.949	0.068

† TN, total N; TP, total P; VS, volatile solids.

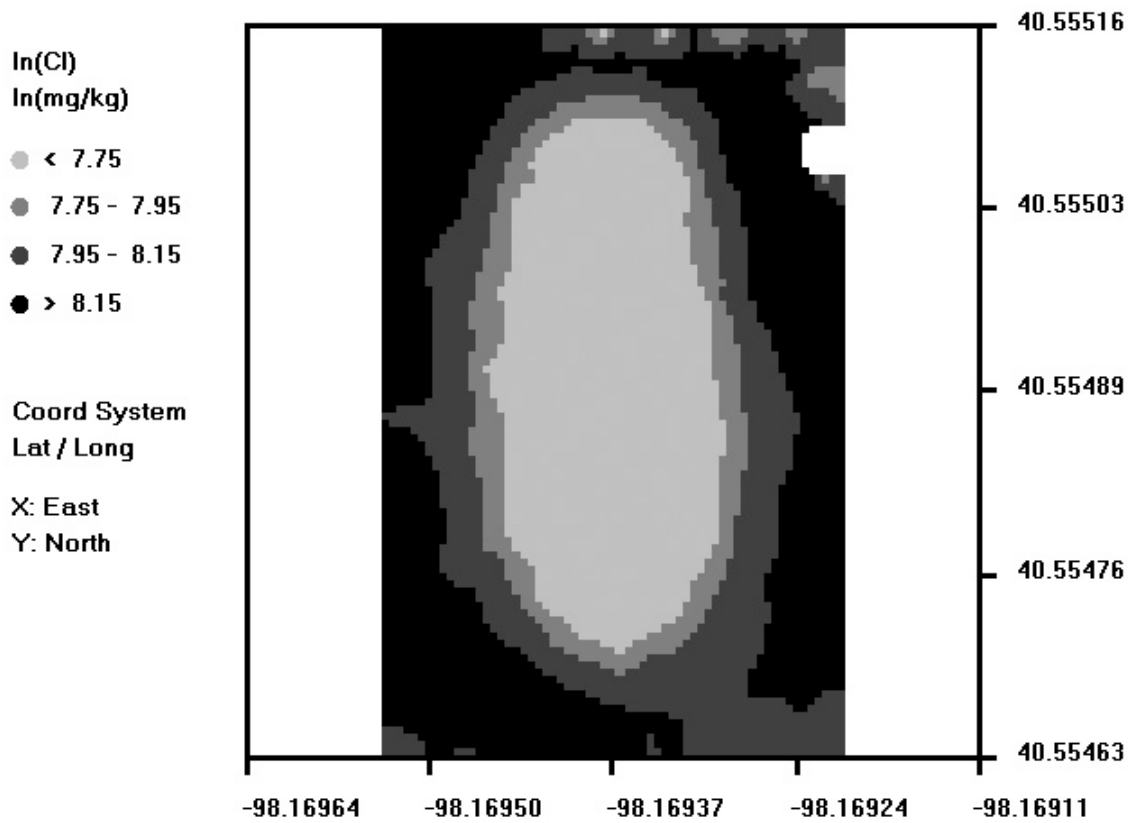


Fig. 4. Predicted spatial $\text{In}(\text{Cl}^-)$ pattern across the feedlot. Note: feed bunk is located at the north end of the pen. Note the light shaded oval denoting the central earth mound.

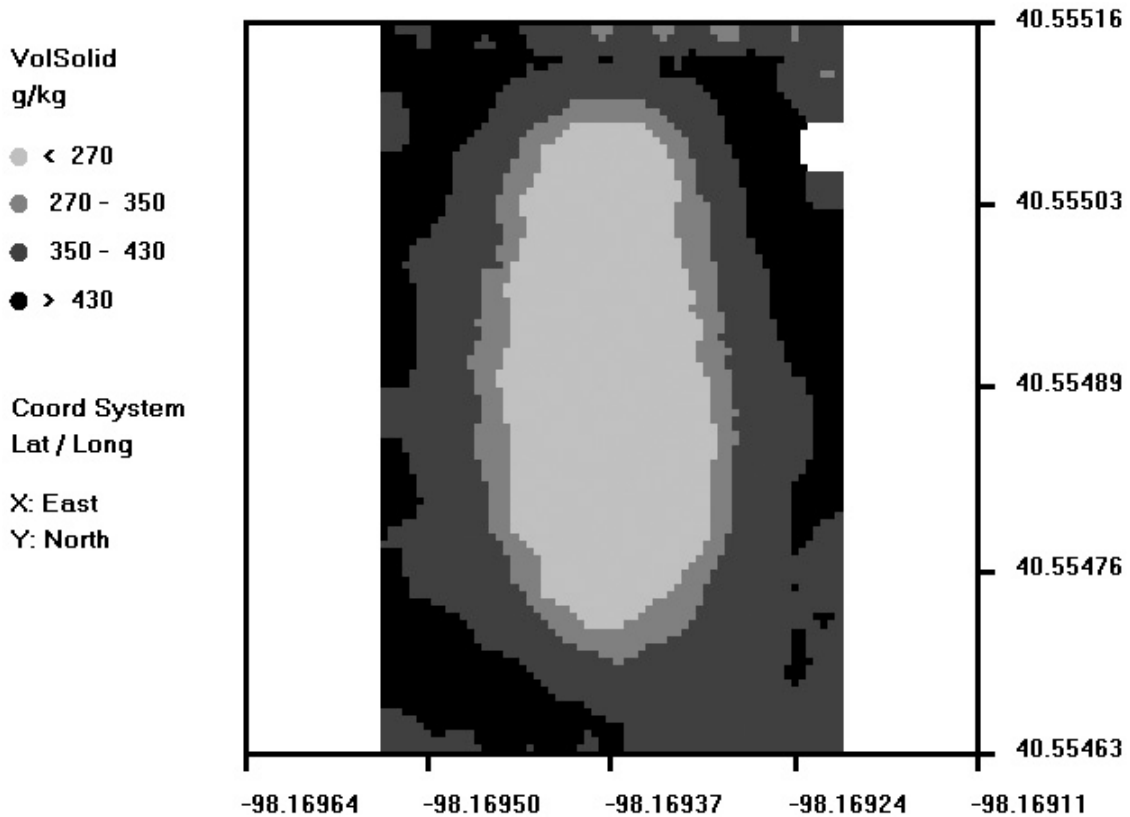


Fig. 5. Predicted spatial volatile solids (VS) pattern across the feedlot. Note: feed bunk is located at the north end of the pen. Note the light shaded oval denoting the central earth mound.

standing can provide researchers with direction for developing management practices for controlling manure's impact on the environment.

Approximately 75% of material cleaned and removed from soil-surfaced feedlot pens is non-volatile (Kissinger et al., 2007). This nonvolatile material is primarily comprised of soil particles. Manure entrained with nonvolatile material is expensive to haul to the field as a fertilizer soil amendment because of the weight associated with these particles. Therefore, agricultural fields closest to feedlots may receive excessive amounts of manure, resulting in N and P accumulation. Recently, regulations have required feedlot operators to identify sufficient land to receive the manure generated by their operations. Because much of the land closest to feedlots have a history of receiving manure, it is either limited or not available as a land resource due to high nutrient levels that exceed regulatory limits. This has forced operators to identify land that is farther away on which to apply the accumulated manure. Based on Fig. 4 and 5, harvesting accumulated manure around the perimeter of the central mound should yield material that is much higher in volatile solids than material that is scraped from the entire area. This nutrient-concentrated material could be economically hauled to fields farther from the feedlot, while the less concentrated material may be more suited to closer fields.

Gases such as NH₃, greenhouse gases, and volatile organic compounds associated with malodor (volatile fatty acids, aromatics, sulfides, amides, and alcohols) emissions from feedlots result from microbial degradation of excreted carbohydrates, fats, and proteins found in accumulated animal manure (Berry et al., 2006; Berry and Miller, 2005; Miller and Berry, 2005; Miller and Woodbury, 2006; Woodbury et al., 2001). The spatial accumulation of these excreted manure nutrients results in zones within the pen that are much more prone to malodorous emissions. Maps illustrating zones of manure nutrient accumulation could be used to focus pen cleaning efforts. Also, these areas could be cleaned more frequently to remove the organic material and reduce the potential for malodorous emissions. Additionally, these zones could be identified and treated with compounds like thymol to inhibit odor production during wet periods when removal is not practical (Varel et al., 2006; Varel and Miller, 2001). The GPS coordinates associated with the mapping technique could be used for precision application of thymol or other antimicrobial compounds to zones with the highest potential for malodorous emissions. This would reduce malodorous emissions

Table 4. Sampling design scores where D optimality (D_{opt}) is a measure of the expected precision of the regression model parameter estimates, V optimality (V_{opt}) is a measure of the expected average prediction error associated with the regression model predictions, and G maximum (G_{max}) is a measure of the expected maximum prediction error of the regression model predictions.

Sampling plan	Sample design optimality score		
	D_{opt}	V_{opt}	G_{max}
Response surface sampling design	1.52×10^{-2}	1.123	1.231
Stratified random sampling	0.22×10^{-2}	1.178	1.989

Table 5. Quadratic regression model summary statistics and parameter estimates for each sampling design; β_0 , β_1 , and β_2 represent quadratic regression model parameter estimates, with the calculated standard errors (SE) shown in parentheses.

Variable†	Design‡	R ²	Root MSE	β_0 (SE)	β_1 (SE)	β_2 (SE)
ln(Cl ⁻)	RSSD	0.953	0.104	1.389 (3.17)	1.650 (1.20)	-0.084 (0.11)
	SRS	0.937	0.086	1.796 (4.91)	1.501 (1.84)	-0.068 (0.17)
TN/1000	RSSD	0.928	1.84	-246.7 (55.5)	88.0 (21.0)	-7.29 (1.96)
	SRS	0.884	1.81	-276.0 (100.2)	97.9 (37.6)	-8.12 (3.52)
TP/1000	RSSD	0.948	0.472	-83.0 (14.3)	29.8 (5.39)	-2.50 (0.50)
	SRS	0.920	0.471	-87.9 (26.1)	31.1 (9.81)	-2.58 (0.92)
VS	RSSD	0.946	3.72	-528.2 (112.4)	186.9 (42.5)	-15.3 (3.97)
	SRS	0.882	4.40	-500.6 (243.8)	173.0 (91.6)	-13.7 (8.56)

† TN, total N; TP, total P; VS, volatile solids.

‡ RSSD, response surface sampling design; SRS, stratified random sampling.

until the manure nutrients could be removed and improve the cost effectiveness of the antimicrobial agent.

Air dispersion models are useful for determining setback distances for new operations or the expansion of existing operations or developing intervention methods for odor control (Nangia et al., 2001). These models rely on input data such as meteorological, topographical, and terrain data, emission rates, and contributing area to predict plume movement and intensity. Emission rates and areas contributing these emissions are difficult to obtain. Many strategies have been used, from simple and inexpensive flux chambers to sophisticated laser-based measurements combined with micrometeorological approaches. These strategies provide estimates but have limitations due to expense, time for data collection, or lack of resolution to identify the point of emission. Mapping manure accumulation zones using EC_a survey data in conjunction with a prediction-based sampling design may provide better estimation of gas emissions from accumulated manure and more accurately identify the contributing area.

CONCLUSIONS

Three different regression model validation tests were used to assess the accuracy and reliability of the fitted model. These tests were used to verify that the regression model estimated using data from just the RSSD sample sites was capable of producing accurate and unbiased predictions at the independently chosen SRS sites. The composite-model *F* test results suggest that the parameter estimates were statistically equivalent across designs. All four joint-prediction *F* tests also exhibited nonsignificant test results. These results indicate that the regression models fit using the RSSD sample data could be used to make accurate and unbiased predictions at the SRS sites. The TN, TP, and VS mean-prediction *t*-tests also produced nonsignificant results.

Table 6. Statistical validation test results; response surface sampling design (RSSD) samples were used as calibration data, stratified random sampling (SRS) samples were used as independent validation sites.

Variable†	Composite <i>F</i> test	Joint prediction <i>F</i> test	Mean prediction <i>t</i> -test
	<i>F</i> score (<i>P</i> > <i>F</i>)	<i>F</i> score (<i>P</i> > <i>F</i>)	<i>t</i> score (<i>P</i> > <i>F</i>)
ln(Cl ⁻)	1.98 (0.136)	0.86 (0.630)	2.14 (0.047)
TN	0.36 (0.785)	0.87 (0.618)	-0.49 (0.628)
TP	0.97 (0.420)	0.99 (0.516)	-0.72 (0.484)
VS	0.50 (0.682)	1.28 (0.307)	-0.48 (0.640)

† TN, total N; TP, total P; VS, volatile solids.

The excellent correlations between the shallow EMI signal data and the $\ln(\text{Cl}^-)$, TN, TP, and VS soil properties suggest that EMI survey data can be effectively used to map spatially variable manure constituents in feedlot pens. Each of the four quadratic regression models was capable of explaining >90% of the constituent sample variations. The fitted regression models were, in turn, used to estimate average accumulation levels and accurately predict the spatial variation in each component. Adaptation of this technique should enable researchers to develop precision management practices to mitigate contamination to the environment from beef feedlots.

The corresponding prediction maps show a pronounced pen design effect on manure accumulation. Maps illustrating zones of manure nutrient accumulation could be used to focus pen cleaning efforts. Also, these areas could be cleaned more frequently to remove this material and reduce the potential for malodorous emissions. These zones could also be identified and treated with compounds like thymol to inhibit odor production during wet periods when removal is not practical. The GPS coordinates associated with the mapping technique could be used for precision application of the thymol or other antimicrobial compounds to zones with the highest potential for malodorous emissions. These efforts would reduce malodorous emissions (until the manure nutrients could be removed) and improve the cost effectiveness of the antimicrobial agent.

APPENDIX

Computation of Optimality Criteria

Let \mathbf{X} represent the design matrix associated with a specific regression model, \mathbf{x}_i represent the regression vector associated with the i th survey location, and p represent the number of parameters in the regression model (including the intercept). Additionally, let n and N represent the number of soil samples and EMI survey sites, respectively. The D -, V -, and G -optimality scores for spatially independent observations are then defined as follows:

$$D_{\text{opt}} = \left| \mathbf{X}^T \mathbf{X} \right| / n^p \quad [\text{A1}]$$

$$V_{\text{opt}} = (1/N) \sum_{i=1}^N \left[1 + \mathbf{x}_i^T (\mathbf{X}^T \mathbf{X})^{-1} \mathbf{x}_i \right] \quad [\text{A2}]$$

and

$$G_{\text{max}} = \max_{i=1, \dots, N} \left[1 + \mathbf{x}_i^T (\mathbf{X}^T \mathbf{X})^{-1} \mathbf{x}_i \right] \quad [\text{A3}]$$

where the function $|\cdot|$ represents the determinant of a matrix. Intuitively, the D_{opt} score measures the expected precision in the regression model parameter estimates; larger scores imply greater precision and a sampling design that maximizes this score is said to be D optimal. The V_{opt} score measures the expected average prediction error associated with the regression model predictions; a lesser score implies a smaller average prediction error and a sampling design that minimizes this score is said to be V optimal. Likewise, the G_{max} score measures the expected maximum prediction error in the regression model predictions; a sampling design that minimizes this score is said to be G optimal.

REFERENCES

Annamalai, K., B. Thien, J. Sweeten, K. Heflin, and L.W. Greene. 2003. Feedlot manure as reburn fuel for NO_x reduction in coal fired plants. p. 203–214. *In*

- Air Pollution from Agricultural Operations III, Proc. Int. Conf. 3rd, Research Triangle Park, NC. 12–15 Oct. 2003. Am. Soc. Agric. Biol. Eng., St. Joseph, MI.
- Auvermann, B.W., A.N. Paila, N. Hiranuma, and J. Bush. 2007. Open-path transmissometry to determine atmospheric extinction efficiency associated with feedyard dust. *In* Proc. Int. Symp. on Air Quality and Waste Management for Agriculture, Broomfield, CO. 16–19 Sept. 2007. ASABE Publ. 701P0907cd. Am. Soc. Agric. Biol. Eng., St. Joseph, MI.
- Banerjee, S., B.P. Carlin, and A.E. Gelfand. 2004. Hierarchical modeling and analysis for spatial data. CRC Press, Boca Raton, FL.
- Berry, E.D., and D.N. Miller. 2005. Cattle feedlot soil moisture and manure content: II. Impact on *Escherichia coli* O157:H7. *J. Environ. Qual.* 34:656–663.
- Berry, E.D., J.E. Wells, S.L. Archibeque, C.L. Ferrell, H.C. Freetly, and D.N. Miller. 2006. Influence of genotype and diet on steer performance, manure odor, and carriage of pathogenic and other fecal bacteria: II. Pathogenic and other fecal bacteria. *J. Anim. Sci.* 84:2523–2532.
- Bierman, S., G.E. Erickson, T.J. Klopfenstein, R.A. Stock, and D.H. Shain. 1999. Evaluation of nitrogen and organic matter balance in the feedlot as affected by level of source of dietary fiber. *J. Anim. Sci.* 77:1645–1653.
- Bremner, J.M. 1996. Nitrogen—Total. p. 1085–1121. *In* D.L. Sparks (ed.) Methods of soil analysis. Part 3. SSSA Book Ser. 5. SSSA, Madison, WI.
- Corwin, D.L., and S.M. Lesch. 2005. Apparent soil electrical conductivity measurements in agriculture. *Comput. Electron. Agric.* 46:11–44.
- Duysen, R., G. Erickson, D. Schulte, and R. Stowell. 2003. Ammonia, hydrogen sulfide and odor emissions from a beef cattle feedlot. ASABE Pap. 034109. Am. Soc. Agric. Biol. Eng., St. Joseph, MI.
- Eigenberg, R.A., J.W. Doran, J.A. Nienaber, R.B. Ferguson, and B.L. Woodbury. 2002. Electrical conductivity monitoring of soil condition and available N with animal manure and a cover crop. *Agric. Ecosyst. Environ.* 88:183–193.
- Eigenberg, R.A., S.M. Lesch, B.L. Woodbury, and J.A. Nienaber. 2008. Geospatial methods for monitoring a vegetative treatment area receiving beef feedlot runoff. *J. Environ. Qual.* 37:S68–S77.
- Eigenberg, R.A., and J.A. Nienaber. 2003. Electromagnetic induction methods applied to an abandoned manure handling site to determine nutrient buildup. *J. Environ. Qual.* 32:1837–1843.
- Eigenberg, R.A., J.A. Nienaber, B.L. Woodbury, and R.B. Ferguson. 2005. Soil conductivity as a measure of soil and crop status: A four-year summary. *Soil Sci. Soc. Am. J.* 70:1600–1611.
- Flesch, T.K., J.D. Wilson, L.A. Harper, and B.P. Crenna. 2005. Estimating gas emission from a farm using an inverse-dispersion technique. *Atmos. Environ.* 39:4863–4874.
- Flesch, T.K., J.D. Wilson, L.A. Harper, R.W. Todd, and N.A. Cole. 2007. Determining ammonia emissions from a cattle feedlot with an inverse dispersion technique. *Agric. For. Meteorol.* 144:139–155.
- Frankenberger, W.T., Jr., M.A. Tabatabai, D.C. Adriano, and H.E. Doner. 1996. Bromine, chlorine, and fluorine. p. 833–867. *In* D.L. Sparks (ed.) Methods of soil analysis. Part 3. SSSA Book Ser. 5. SSSA, Madison, WI.
- Frecks, G.A., and C.B. Gilbertson. 1974. The effect of ration on engineering properties of beef cattle manure. *Trans. ASAE* 17:383–387.
- Gilbertson, C.B., J.R. Ellis, J.A. Nienaber, T.M. McCalla, and T.J. Klopfenstein. 1975. Properties of manure accumulations from Midwest beef cattle feedlots. *Trans. ASAE* 18:327–330.
- Haining, R. 1990. Spatial data analysis in the social and environmental sciences. Cambridge Univ. Press, Cambridge, UK.
- Ham, J.M., and K.A. Baum. 2007. Measuring ammonia fluxes from cattle feedlots using time-averaged relaxed eddy accumulation. *In* Proc. Int. Symp. on Air Quality and Waste Management for Agriculture, Broomfield, CO. 16–19 Sept. 2007. ASABE Publ. 701P0907cd. Am. Soc. Agric. Biol. Eng., St. Joseph, MI.
- Harper, L.A., O.T. Denmead, J.R. Freney, and F.M. Byers. 1999. Direct measurements of methane emissions from grazing and feedlot cattle. *J. Anim. Sci.* 77:1392–1401.
- Haskard, K.A., B.R. Cullis, and A.P. Verbyla. 2007. Anisotropic Matérn correlation and spatial prediction using REML. *J. Agric. Biol. Environ. Stat.* 12:147–160.
- Isaaks, E.H., and R.M. Srivastava. 1989. An introduction to applied geostatistics. Oxford Univ. Press, New York.
- Kissinger, W.F., R.K. Koelsch, G.E. Erickson, and T.J. Klopfenstein. 2007. Characteristics of manure harvested from beef cattle feedlots. *Appl. Eng. Agric.* 23:357–365.
- Kuo, S. 1996. Phosphorus. p. 869–919. *In* D.L. Sparks (ed.) Methods of soil analysis. Part 3. SSSA Book Ser. 5. SSSA, Madison, WI.

- Kyoung, S.R., P.G. Hunt, M.H. Johnson, A.A. Szogi, and M.B. Vanotti. 2007. Path integrated optical remote sensing technique to estimate ammonia and methane emissions from CAFOs. *In* Proc. Int. Symp. on Air Quality and Waste Management for Agriculture, Broomfield, CO. 16–19 Sept. 2007. ASABE Publ. 701P0907cd. Am. Soc. Agric. Biol. Eng., St. Joseph, MI.
- Lesch, S.M. 2005. Sensor-directed response surface sampling designs for characterizing spatial variation in soil properties. *Comput. Electron. Agric.* 46:153–180.
- Lesch, S.M., and D.L. Corwin. 2008. Prediction of spatial soil property information from ancillary sensor data using ordinary linear regression: Model derivations, residual assumptions and model validation tests. *Geoderma* 148:130–140.
- Lesch, S.M., J.D. Rhoades, and D.L. Corwin. 2000. ESAP-95 Version 2.10R: User manual and tutorial guide. Res. Rep. 146. U.S. Salinity Lab., Riverside, CA.
- Lesch, S.M., D.J. Strauss, and J.D. Rhoades. 1995a. Spatial prediction of soil salinity using electromagnetic induction techniques: 1. Statistical prediction models: A comparison of multiple linear regression and cokriging. *Water Resour. Res.* 31:373–386.
- Lesch, S.M., D.J. Strauss, and J.D. Rhoades. 1995b. Spatial prediction of soil salinity using electromagnetic induction techniques: 2. An efficient spatial sampling algorithm suitable for multiple linear regression model identification and estimation. *Water Resour. Res.* 31:387–398.
- McGinn, S.M., H.H. Janzen, and T. Coates. 2003. Atmospheric ammonia, volatile fatty acids, and other odorants near beef feedlots. *J. Environ. Qual.* 32:1173–1182.
- Meisinger, J.J., A.M. Lefcourt, and R.B. Thompson. 2001. Construction and validation of small mobile wind tunnels for studying ammonia volatilization. *Appl. Eng. Agric.* 17:375–381.
- Miller, D.N., and E.D. Berry. 2005. Cattle feedlot soil moisture and manure content: I. Impacts on greenhouse gases, odor compounds, nitrogen losses, and dust. *J. Environ. Qual.* 34:644–655.
- Miller, D.N., and B.L. Woodbury. 2006. A solid-phase microextraction chamber method for analysis of manure volatiles. *J. Environ. Qual.* 35:2383–2394.
- Müller, W.G. 2001. Collecting spatial data: Optimum design of experiments for random fields. 2nd ed. Physica-Verlag, Heidelberg, Germany.
- Myers, R.H. 1986. Classical and modern regression with applications. Duxbury Press, Boston.
- Myers, R.H., and D.C. Montgomery. 2002. Response surface methodology: Process and product optimization using designed experiments. 2nd ed. John Wiley & Sons, New York.
- Nangia, V., K.A. Janni, and L.D. Jacobson. 2001. Assessing feedlot odor impacts with OFFSET and GIS. ASABE Pap. 014044. Am. Soc. Agric. Biol. Eng., St. Joseph, MI.
- Nelson, D.W., and L.E. Sommers. 1996. Total carbon, organic carbon, and organic matter. p. 961–1010. *In* D.L. Sparks (ed.) *Methods of soil analysis*. Part 3. SSSA Book Ser. 5. SSSA, Madison, WI.
- Priyadarsan, S., K. Annamalai, J.M. Sweeten, S. Mukhtar, and M.T. Hotzapple. 2004. Fixed-bed gasification of feedlot manure and poultry litter biomass. *Trans. ASAE* 47:1689–1696.
- Rhoades, J.D., F. Chanduvi, and S.M. Lesch. 1999. Soil salinity assessment: Methods and interpretation of electrical conductivity measurements. FAO Irrig. Drain. Pap. 57. FAO, Rome.
- Schabenberger, O., and C.A. Gotway. 2005. Statistical methods for spatial data analysis. CRC Press, Boca Raton, FL.
- Shapiro, S.S., and M.B. Wilk. 1965. An analysis of variance test for normality (complete samples). *Biometrika* 52:591–611.
- Sweeten, J.M., R.P. Egg, E.L. Reddell, V. Varani, and S. Wilcox. 1985. Characteristics of cattle feedlot manure in relation to harvesting practices. p. 329–337. *In* Agricultural Waste Utilization and Management. Proc. Int. Symp. on Agric. Waste, 5th, Chicago. 16–17 Dec. 1985. ASAE Publ. 13-85. Am. Soc. Agric. Eng., St. Joseph, MI.
- Sweeten, J.M., K. Heflin, K. Annamalai, B.W. Auvermann, F.T. McCollum, and D.B. Parker. 2006. Combustion-fuel properties of manure or compost from paved vs. un-paved cattle feedlots. ASABE Pap. 064143. Am. Soc. Agric. Biol. Eng., St. Joseph, MI.
- Tiefelsdorf, M. 2000. Modeling spatial processes: The identification and analysis of spatial relationships in regression residuals by means of Moran's *I*. Springer-Verlag, New York.
- Todd, R.W., N.A. Cole, L.A. Harper, and T.K. Flesch. 2008. Ammonia emissions from a beef cattle feedyard on the southern High Plains. *Atmos. Environ.* 42:6797–6805.
- Todd, R.W., N.A. Cole, L.A. Harper, T.K. Flesch, and B.H. Baek. 2005. Ammonia and gaseous nitrogen emissions from a commercial beef cattle feedyard estimated using the flux-gradient method and N:P ratio analysis. *In* State of the Science: Animal Manure and Waste Management Symp., San Antonio, TX. 4–7 Jan. 2005 [CD-ROM]. North Carolina State Univ., Raleigh.
- Upton, G., and B. Fingleton. 1985. Spatial data analysis by example. John Wiley & Sons, New York.
- Varel, V.H., and D.N. Miller. 2001. Plant-derived oils reduce pathogen and gaseous emissions from stored cattle waste. *Appl. Environ. Microbiol.* 67:1366–1370.
- Varel, V.H., D.N. Miller, and E.D. Berry. 2006. Incorporation of thymol into corn cob granules for reduction of odor and pathogens in feedlot cattle waste. *J. Anim. Sci.* 84:481–487.
- Wackernagel, H. 1998. Multivariate geostatistics. 2nd ed. Springer-Verlag, Berlin.
- Woodbury, B.L., D.N. Miller, J.A. Nienaber, and R.A. Eigenberg. 2001. Seasonal and spatial variations of denitrifying enzyme activity in feedlot soil. *Trans. ASAE* 44:1635–1642.